Pflugers Arch - Eur J Physiol
DOI 10.1007/s00424-013-1288-y

MOLECULAR AND CELLULAR MECHANISMS OF DISEASE

Vascular endothelium leaves fingerprints on the surface of erythrocytes

Hans Oberleithner

Received: 26 March 2013 / Revised: 15 April 2013 / Accepted: 22 April 2013
© Springer-Verlag Berlin Heidelberg 2013

Abstract Gliding of red blood cells (RBC) through blood vessels is mediated by the negatively charged glycocalyx located on the surfaces of both RBC and endothelial cells (EC). In various vasculopathies, EC gradually lose this protective surface layer. As a consequence, RBC come into close physical contact with the vascular endothelium. It is hypothesized that the RBC glycocalyx could be adversely affected by a poor EC glycocalyx. This hypothesis was tested by evaluating the RBC and EC surface layers with atomic force microscopy techniques. In the first series of experiments, EC monolayers grown in culture were exposed to rhythmic drag forces exerted from a blood overlay (drag force treatment), and thereafter, the EC surface was investigated in terms of thickness and adhesiveness. In the second series, the glycocalyx of the EC monolayers was disturbed by enzymatic cleavage of negatively charged heparan sulfates before drag force treatment, and thereafter, the RBC surface was evaluated. In the third series, the RBC glycocalyx of the blood overlay was enzymatically disturbed before drag force treatment, and thereafter, the EC surface was evaluated. A strong positive correlation between the RBC and EC surface properties was found (r^2=0.95). An enzymatically affected EC glycocalyx lead to the shedding of the RBC glycocalyx and vice versa. It is concluded that there is physical interaction between the blood and endothelium. Apparently, the RBC glycocalyx reflects properties of the EC glycocalyx. This observation could have a significant impact on diagnosis and treatment of cardiovascular diseases.

H. Oberleithner (✉)
Institute of Physiology II, University of Münster,
Robert-Koch-Str. 27b,
48149 Münster, Germany
e-mail: oberlei@uni-muenster.de

Keywords Erythrocyte glycocalyx · Heparan sulfate · Endothelial glycocalyx · Atomic force microscopy

Introduction

Blood flow through the vascular system is a low-friction process due to the fact that the surface of the endothelium lining the vessel walls is covered by a proteoglycan layer, the endothelial glycocalyx (eGC) [29, 37, 45]. This gel-like polymer, rich in water and anionic charges such as heparan sulfate residues, forms a functional cushion between the red blood cells (RBC) and the endothelial plasma membrane. The eGC is a several hundreds of nanometers in height, serving as a barrier in which macromolecules such as albumin are embedded [36]. Thus, the eGC creates a delicate nanoenvironment which participates in the regulation of blood flow [20, 33, 42] and vascular permeability [1, 3, 7, 27]. Due to the anionic properties of the eGC, there are negative electrostatic forces which repel negatively charged RBC from getting too close to the endothelial plasma membrane. The electrical surface properties explain the low adhesiveness of RBC to endothelium and the virtually frictionless slipping of RBC through the blood vessels [20].

However, there are pathophysiological states such as metabolic syndrome [23], inflammatory processes [4, 19], and excess sodium intake [26] that severely damage the eGC. Under such conditions, the eGC can gradually shrink and lose its negative charges. A shedded eGC could lead to an intimate physical contact between RBC and endothelial cells (EC). Thus, circulating RBC will exert higher drag forces when slipping through narrow blood vessels [20], and as a consequence, the RBC glycocalyx (rGC) will suffer from this "mechanical" interaction and gradually shrink. This hypothesis was tested in an in vitro approach where vascular endothelium was exposed to the drag forces of a

Published online: 11 May 2013

blood overlay, and where, in an experimental step before, either the eGC or the rGC has been enzymatically manipulated. It was found that rGC and eGC influence each other when either one of them is in a poor condition.

Methods

RBC–EC interaction experiments and atomic force microscopy imaging

Endothelial monolayers (Eahy629 cell line cultured on the bottom of 75-cm^2 culture flasks [8, 17, 18]) were exposed, over a time period of 5 h, to 5 ml of whole blood (heparinized Monovettes, Sarstedt Company, Sarstedt, Germany) taken from volunteers. The flasks were continuously rocked on a shaker (4 shifts per min, 7° angle) placed in a cell culture incubator (37 °C, 5 % CO_2) so that the RBC can physically interact with the surface of the endothelial cell layer. Using the culture flasks as mentioned above, a mean RBC velocity of about 30 m/h and a mean total RBC travel distance of 150 m (over 5 h) can be calculated. Unfortunately, with this experimental approach, we cannot quantify specific forces that occur between RBC and the endothelial surface. Thus, in pilot experiments, we used "RBC hemolysis" as a parameter to adjust the experimental settings (flask tilt angle, shifts per minute, and shaking time), i.e., a setting was chosen where significant RBC hemolysis just did not yet occur. This procedure is called "drag force treatment."

Three series of experiments were performed (Fig. 1). In the first series, intact EC monolayers ("intact" EC) were overlaid with whole blood (intact RBC) and exposed to drag force treatment. Thereafter, the blood overlay was harvested and centrifuged, and RBC were resuspended in buffered electrolyte solution composed of the following: 140 mM NaCl, 5 mM KCl, 1 mM $MgCl_2$, 1 mM $CaCl_2$, and 10 mM *N*-2-hydroxyethylpiperazine-*N*′-2-ethanesulfonic acid (HEPES), pH 7.4. The dilution factor (RBC/buffer) was about 1/1,000. A small sample (50 μl) of this solution was spread on a poly-L-lysine-coated glass cover slip, and the RBC were allowed to firmly stick to the coated glass surface. Then, RBC were gently fixed with 0.1 % glutaraldehyde. In a next step, RBC were imaged in HEPES buffer by using an atomic force microscope (Multimode® Atomic Force Microscopy (AFM) with a feedback-controlled heating device, Bruker Corporation, Santa Barbara, CA, USA) [25, 32]. In order to characterize the RBC glycocalyx properties after the drag force treatment, differential images were achieved (Fig. 2). In detail, RBC were imaged before (image A) and 30 min after adding 2 Sigma-U/ml heparinase (image B; heparinase I, Sigma-Aldrich Chemie, Taufkirchen, Germany). Then, the two images were electronically subtracted from each other ($A-B$) resulting in a differential image C. Since the heparinase only cleaves the heparan sulfate residues of the glycocalyx while leaving the fixed RBC unaffected, this differential image C shows selectively the heparinase-sensitive portion of the glycocalyx. Similarly, intact endothelial cells of the fixed EC monolayer (same fixation as described above for RBC), after being exposed to the drag force treatment, were imaged before and after heparinase application (Fig. 2). To get access to the EC surface, the culture flasks were sawed, and a small piece of the flask bottom (about 1 cm^2) was covered with the glutaraldehyde-fixed EC monolayer used for AFM imaging.

In the second series of experiments, the negatively charged heparan sulfate residues of the eGC were enzymatically removed by heparinase, resulting in "damaged" EC. Then, the drag force experiment was performed, and the

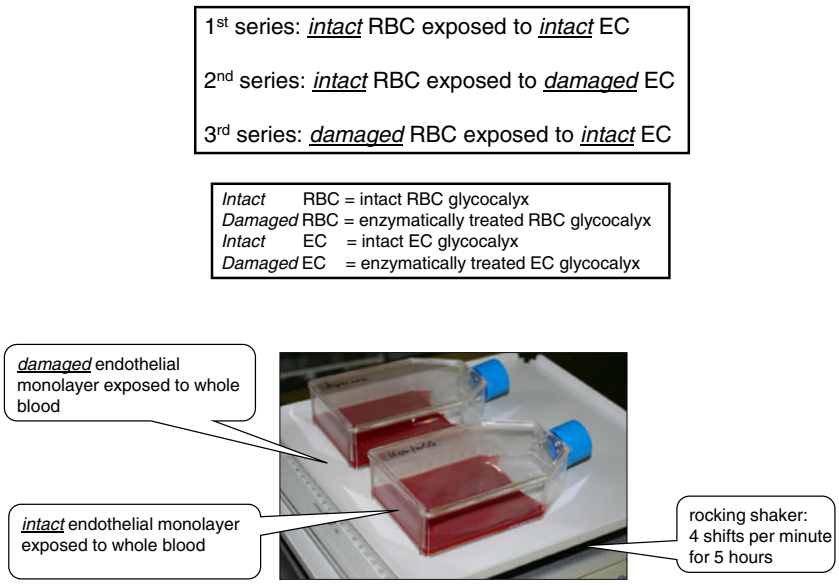

Fig. 1 Drag force treatment. Three experimental series were designed. (1) Intact endothelium is exposed to intact RBC. (2) Intact RBC are exposed to damaged EC. (3) Damaged RBC are exposed to intact EC. *Intact* native RBC or EC. *Damaged* heparinase-pretreated RBC or EC

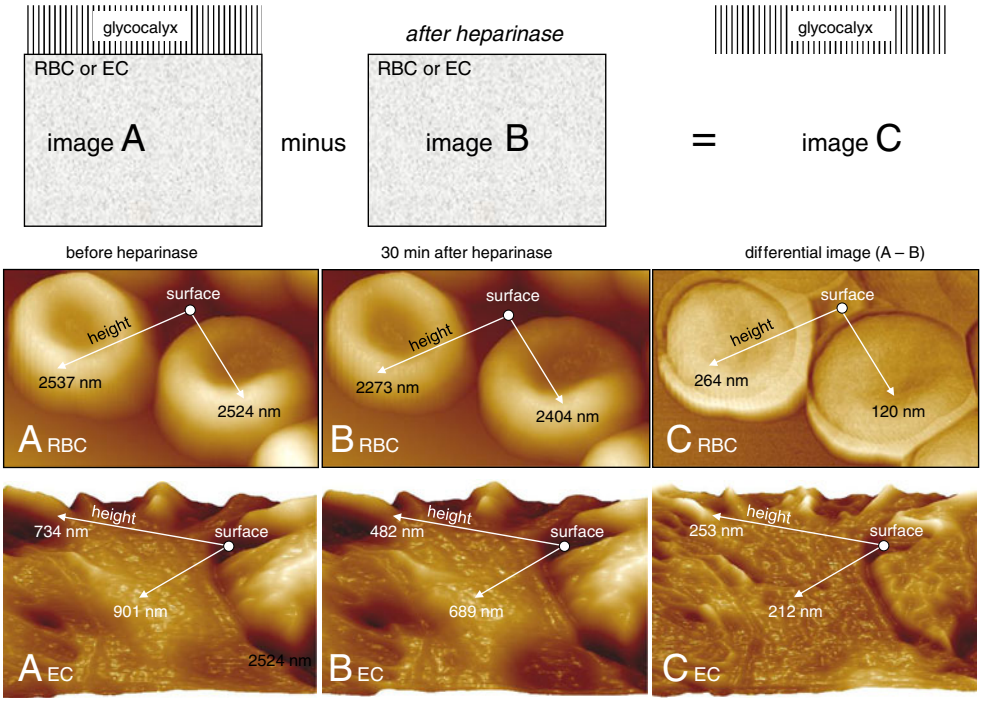

Fig. 2 Imaging the glycocalyx of red blood cells (*RBC*) and endothelial cells (*EC*). The *upper row* shows the experimental protocol. The *middle row* displays RBC scans, and the *lower row*, EC scans. In a first step, RBC/EC are imaged (images *A*). Then, heparinase is added, and RBC/EC images are generated after 30 min (images *B*). In off-line mode, the respective images are electronically subtracted from each other which results in a differential image (image *C*) exhibiting the heparinase-sensitive portion of the glycocalyx. For analyses, a reference point on the glass surface is chosen, from which individual height measurements of specific locations on the RBC/EC surface can be made. The *numbers* in the individual images are height values (in nanometer) obtained at corresponding RBC/EC sites. The annular collar shown in the RBC differential image (image C_{RBC}) is probably an artifact due to AFM tip convolution

RBC harvested from the blood overlay were studied as described above (Figs. 1 and 2).

In the third series of experiments, blood was centrifuged, and RBC were suspended in HEPES buffer and exposed to heparinase for 60 min. Then, damaged RBC were again centrifuged and suspended in the respective plasma, maintaining the original hematocrit. This (modified) blood was used as the fluid overlay for the drag force treatment of intact EC monolayers. Finally, the same protocol as described above was used for EC fixation, acute heparinase treatment, and EC imaging.

AFM adhesion measurements

Adhesion (pull-off) forces between the negatively charged silica particle tip (1 μm SiO_2 spheres, spring constant 0.01–0.02 N/m, Novascan, Ames, IA, USA) and the glycocalyx covering RBC or EC were measured on glutaraldehyde (0.1 %)-fixed cells in HEPES buffer. Force–distance cycles were performed, and interaction forces were determined using the SPIP software (Image Metrology A/S, Horsholm, Denmark). Loading forces were in the range of 400 pN. At least 5 force–distance cycles/cell were performed at about 0.2 Hz (1 cycle per 5 s), and the pull-off forces were derived from five retraction curves (of an individual cell) and averaged. Using this protocol, 20 RBC and 20 EC were analyzed (n=20).

All AFM experiments (imaging and adhesion measurements) were performed at the same conditions, namely, in HEPES-buffered saline at pH 7.4 and 37 °C. The saline buffer was always supplemented with 1 % fetal calf serum (PAA Clone, Coelbe, Germany). The addition of serum is necessary for maintaining a functional glycocalyx [26]. Though cells were fixed, the glycocalyx still responds to heparinase I treatment (2 Sigma-U/ml in all experiments) when the temperature is maintained at 37 °C.

Statistics Some of the data are shown as mean values ± standard error of the mean (SEM). Significance of differences was evaluated by the paired or unpaired Student's t test if applicable. The overall significance level is P=0.05 or less.

Results

In order to get quantitative data of the RBC and EC surface layers, cells were imaged before (image A in Fig. 2) and shortly after (image B in Fig. 2) enzymatic removal of

heparan sulfate residues. The respective differential images (image C in Fig. 2) disclose the glycocalyx, or more precisely, that portion of the glycocalyx which was cleaved by heparinase I. The cells were fixed by glutaraldehyde before the cleavage measurements and scanned in fluid. This experimental approach has two advantages: on the one hand, the overall shape of the RBC/EC remains unaffected by the scan forces (i.e., no changes of the fixed (rigid) cell body) and insensitive to heparinase treatment. On the other hand, the glycocalyx (i.e., the gel-like surface layer) of the fixed cells is still sensitive to enzyme treatment. Thus, the difference between the images generated before and after enzyme treatment is made up only by changes of the glycocalyx. Therefore, the differential images ($A-B=C$, Fig. 2) should reflect the surface layers removed by the enzyme treatment. The time course of the glycocalyx breakdown after addition of heparinase was monitored in six individual RBC and EC (Fig. 3a, b). Glycocalyx breakdown due to the enzymatic cleavage of the heparan sulfate residues is indicated by the change in the respective RBC/EC heights after heparinase treatment. Furthermore, adhesion forces were measured by means of a negatively charged glass particle AFM tip before (control) and 20 min after heparinase treatment (Fig. 3c, d). In both cell types, RBC and EC adhesion forces significantly increased, indicating that the surfaces lost negative charges (i.e., heparan sulfate residues) when treated with heparinase. These observations led us to test the "physical" cross talk between eGC and rGC.

Monolayers of endothelial cells cultured in flasks were exposed to whole blood for 5 h (Fig. 1). As described in "Methods," the flasks were mounted on a rocking table dragging the blood rhythmically forth and back across the endothelial surface (drag force treatment). Rhythm and tilt angle were adjusted so that this maneuver should generate maximal drag forces exerted from the blood overlay onto the EC monolayer (see "Methods" for details). After this treatment, rGC and eGC were analyzed by atomic force microscopy methods. Figure 4 shows the results obtained in RBC. RBC volume (due to the loss of heparin sulfate residues) decreases in response to heparinase treatment. The magnitude of this decrease, however, is quantitatively different, depending on whether the RBC were harvested from an endothelium pretreated with heparinase (damaged endothelium) or harvested from an intact EC monolayer (intact

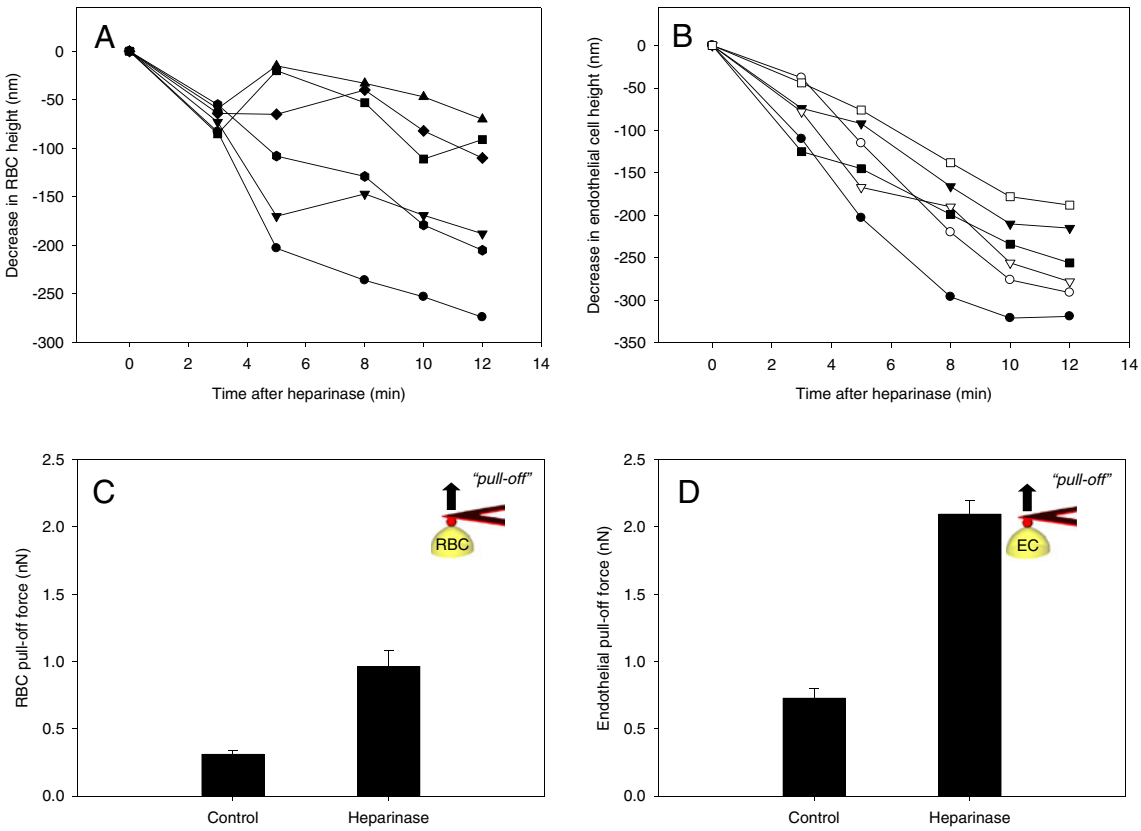

Fig. 3 Height and adhesion force changes in RBC and EC. **a** Changes of individual RBC heights (in nanometer) in response to heparinase. **b** Changes of individual EC heights (in nanometer) in response to heparinase. *Each point* represents the mean value of ten height measurements at different sites of one individual red blood cell. **c** Mean values (n=20, ±SEM) of RBC pull-off forces (in nanonewton) before (control) and 20 min after heparinase treatment (P<0.01). **d** Mean values (n=20, ±SEM) of EC pull-off forces (in nanonewton) before (control) and 20 min after heparinase treatment (P<0.01). *Insets* in **c** and **d** illustrate the experimental procedure

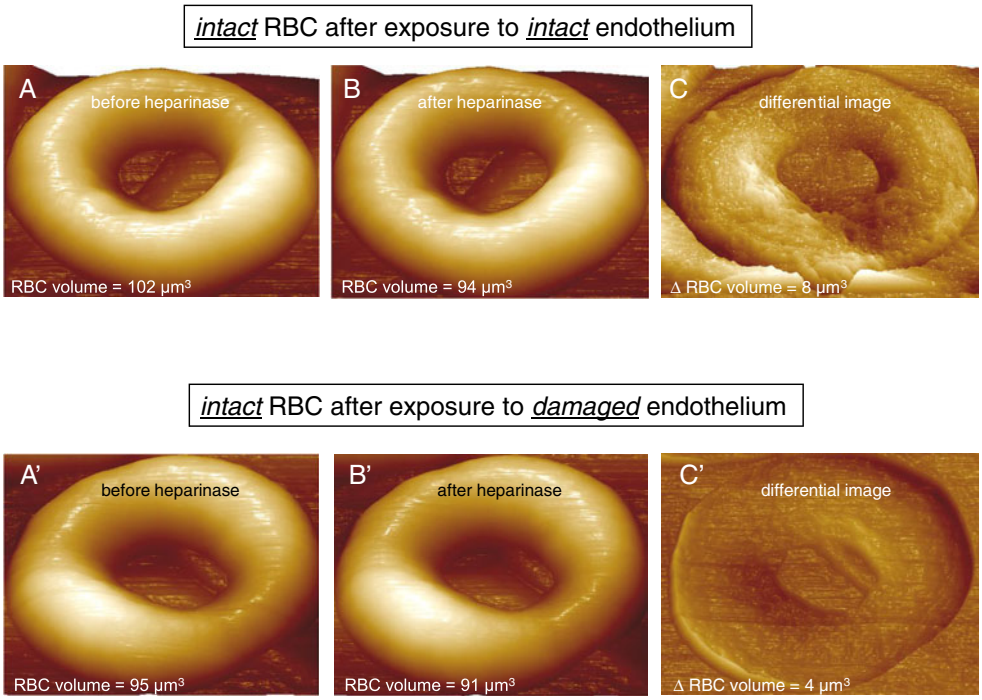

Fig. 4 RBC imaging after physical contact with the EC monolayer. An individual red blood cell was imaged before (*A*/*A*′) and 30 min after (*B*/*B*′) heparinase treatment. The heparinase-sensitive portion of the RBC glycocalyx (given as Δvolume) was identified (differential images *C*/*C*′) after exposure of intact RBC to either intact endothelium (*upper row*) or damaged endothelium (*lower row*)

endothelium). RBC exposed to damaged endothelium lose more glycocalyx (i.e., heparin sulfate) during the drag force treatment as compared to RBC exposed to intact endothelium. In another series of experiments, whole blood containing damaged RBC (i.e., RBC pretreated with heparinase) was exposed to intact endothelium following the same experimental protocol. Now, the EC surfaces were evaluated (Fig. 5). EC volume decreases in response to heparinase treatment. However, in analogy to the experiments described above, the glycocalyx of the (initially) intact endothelium shrinks, when exposed to damaged RBC during the drag force treatment. This shrinkage is quantitatively more prominent compared to the experiment where intact endothelium was exposed to intact RBC. Figure 6 shows an analysis of the glycocalyx height values. It becomes apparent that a damaged partner (either damaged

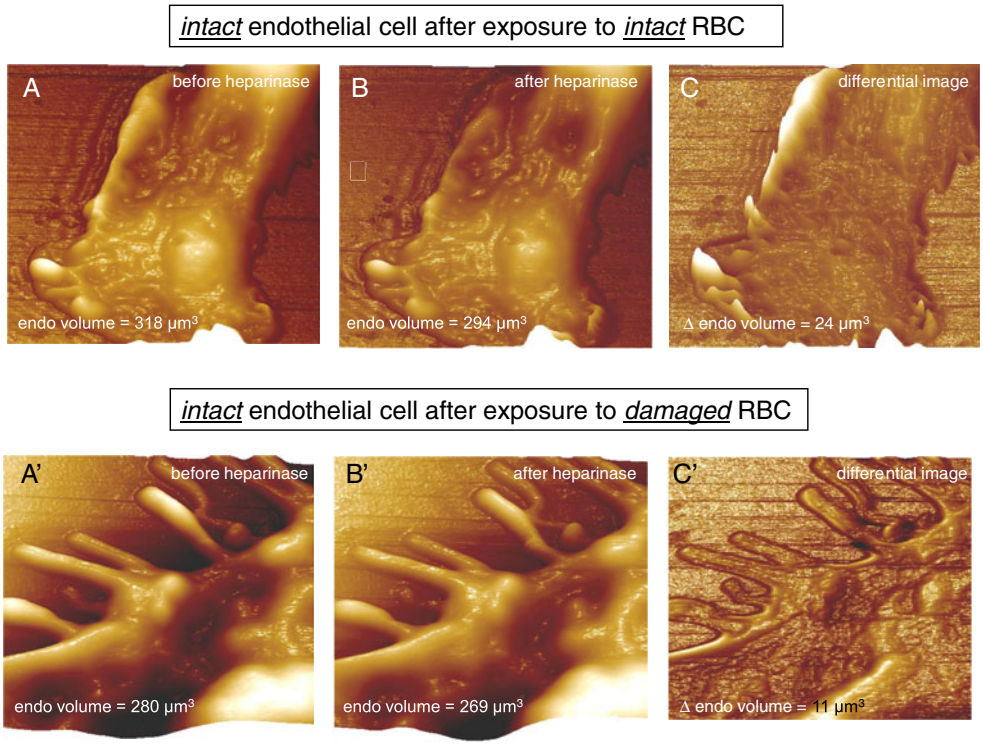

Fig. 5 EC imaging after physical contact with the whole blood. Part of an individual EC was imaged before (*A*/*A*′) and 30 min after (*B*/*B*′) heparinase treatment. The heparinase-sensitive portion of the EC glycocalyx (given as Δvolume) was identified (differential images *C*/*C*′) after exposure of intact endothelium to either intact RBC (*upper row*) or damaged RBC (*lower row*)

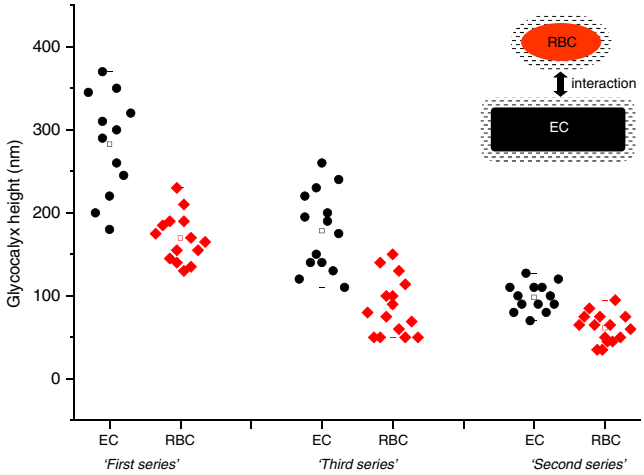

Fig. 6 Glycocalyx height measurements in RBC and EC after the respective drag force treatments. *Each data point* represents a single measurement taken from the respective differential images (C_{RBC} and C_{EC}). The terms "first series," "second series," and "third series" refer to the nomenclature introduced in Fig. 1 and described in the "Methods" section. In short, in the first series, intact endothelium is exposed to intact RBC; in the second series, intact RBC are exposed to damaged EC; and in the third series, damaged RBC are exposed to intact EC. *Intact*, native RBC or EC. *Damaged*, heparinase-pretreated RBC or EC. The mean values of the RBC and EC heights of the second and third series were significantly different ($P<0.01$) when compared with the respective mean values of the first series

RBC or damaged EC) alters the surface properties of the (initially) intact partner. Figure 7 summarizes the height values of the RBC/EC "pairs." There is a strong correlation between rGC and eGC height values. The data indicate that rGC and eGC physically interact with each other. It appears likely that the endothelial surface layer leaves its

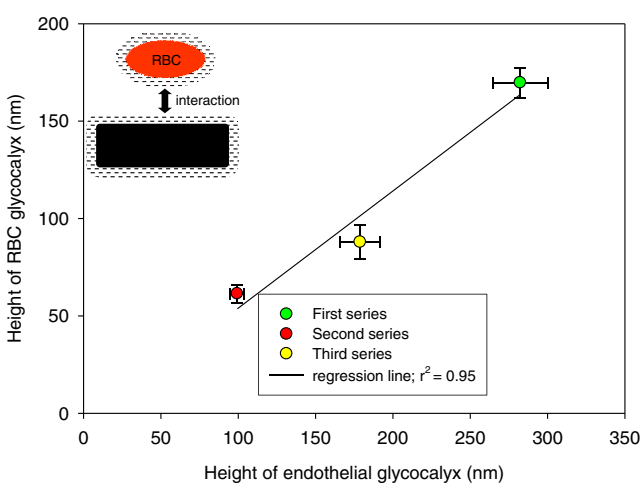

Fig. 7 Relationship between the respective heights of EC and RBC. The terms first series, second series, and third series refer to the nomenclature introduced in Fig. 1 and described in the "Methods" section. In short, in the first series, intact endothelium is exposed to intact RBC; in the second series, intact RBC are exposed to damaged EC; and in the third series, damaged RBC are exposed to intact EC. *Intact*, native RBC or EC. *Damaged*, heparinase-pretreated RBC or EC

"fingerprints" on the RBC surface and vice versa. Given are mean values +/- SEM (number of single measurements 12-15; see figure 6).

Discussion

The luminal wall of all blood vessels is lined by a thin cell monolayer, the vascular endothelium. This EC layer serves a number of important functions. It is (a) a selective mechanical barrier between blood and tissue [15, 41], (b) a biochemically highly active cell layer in the control of blood clotting processes [40], and (c) a key regulator of vascular smooth muscle tone [21]. The luminal EC surface is covered by a gel-like anionic biopolymer, the endothelial glycocalyx [29, 31, 46]. This negatively charged surface layer, hundreds of nanometer in thickness, prevents the unspecific adhesion of circulating blood cells, slows down blood flow in the capillary system [30], and selectively controls endothelial permeability [17, 24].

There is evidence that the endothelial glycocalyx is not homogeneous in structure. Three glycosaminoglycans, namely, heparan sulfate, chondroitin sulfate, and hyaluronan, participate in the control of adhesion processes, blood flow, and vascular permeability. While chondroitin sulfate and hyaluronan are located close to the endothelial plasma membrane, heparan sulfate is supposed to be located more at the "edge" of the glycocalyx directly facing the blood stream [9]. Thus, the negatively charged heparan sulfates, located right at the interface between "moving blood" and "resting vessel wall," are most likely key elements signaling changes in shear stress, blood flow, and composition of the blood to the underlying endothelial monolayer [45]. This explains the severe medical problems that can occur when the glycocalyx is damaged. Among them are vascular permeability changes during inflammatory processes [3] of endothelial dysfunction in chronic kidney failure [43] and atherothrombosis [23].

One of the major functions of the glycocalyx, and in particular of the negatively charged heparan sulfate residues directly facing the streaming blood, is to prevent RBC from getting attached to the endothelial surface. Similarly as the vascular endothelium, erythrocyte membranes are covered by a glycocalyx which, besides sialic acid [6], also contains negatively charged heparan sulfates [5, 16, 44]. Thus, a poor adhesiveness of RBC to EC is explained by electrostatic repulsive forces caused by the zeta potential as described for RBC [13]. Over the 120 days life span of an individual red blood cell, the erythrocyte membrane gradually ages as indicated by a decrease in glycocalyx thickness [11, 22]. This is not unexpected because RBC lack nuclei and thus cannot compensate any losses of surface molecules in the long run. In addition, RBC mechanical stress is particularly high during turbulent blood flow at bifurcations of large arteries and during slipping through the narrow capillaries. The present study indicates that

rGC and eGC "on contact" may influence each other. EC with a charge-depleted surface lead to RBC with similar properties and vice versa. The reason for this adaptation process is most likely a mechanical interaction between RBC and EC [10, 35]. In vivo, this is caused by the streaming blood. In the present in vitro study, this was simulated by rhythmically rocking the culture flasks (i.e., drag force treatment).

The atomic force microscope [2] is a suitable tool for imaging the surface layer and measuring adhesion forces of RBC and EC. A technical prerequisite for imaging glycocalyx thickness, volume, and adhesion properties is that although cells have been fixed (glutaraldehyde) prior to the experiments, the heparan sulfates of the surface layers can be still enzymatically cleaved. In other words, the (dead) cell body remains unaffected, while the glycocalyx can still be manipulated. Such a scenario allows differential imaging (i.e., generating "net" images by the electronic subtraction of two corresponding images) and, thus, identification of the cleaved parts of the glycocalyx. Using this approach, the height resolution (*z*-axis) is in the range of 10 nm which is at least ten times above the resolution of confocal fluorescence imaging [48]. Besides, imaging atomic force microscopy was used as a mechanosensor similar as described previously [47]. By using negatively charged mechanosensors made of pure silica, the cleavage of heparan sulfates can be followed continuously as indicated by changes in adhesion probability. Taken together, atomic force microscopy provides information on glycocalyx thickness, shape, and, indirectly, electrical charge in a reasonable resolution.

The "cross talk" between RBC and EC could have relevance for the progression of cardiovascular diseases and in medical diagnostics. Extrapolating the in vitro results to in vivo conditions, it can be assumed that a vicious cycle could start when either RBC or EC surface layers are damaged by any reason. There is supporting evidence that "poor" vascular function is often found in parallel with poor RBC conditions. Uremic patients suffer from endothelial dysfunction, loss of glycocalyx barrier [43], and anemia. Although the latter is explained by a lack of renal erythropoietin, RBC membranes were found abnormal, and RBC life span reduced [38, 39]. A similar parallelism (i.e., endothelial dysfunction combined with RBC abnormalities) can be observed in sepsis [34], genetic hypertension [28], sickle cell anemia [12], and malaria [44]. These observations support—though do not prove—the hypothesis that the physical interaction between erythrocyte and endothelial surfaces becomes relevant in pathophysiological states, i.e., a damaged endothelial surface damages the erythrocyte surface and vice versa.

The observation that the RBC surface reflects the condition of the corresponding endothelial surface could be also relevant for medical diagnostics. It is known for decades that the erythrocyte sedimentation rate (ESR) inversely correlates with the RBC zeta potential [14]. An increased ESR corresponds to a decrease in the RBC zeta potential commonly used as an unspecific indicator for ongoing inflammatory processes of a patient. Regarding the current in vitro data, it is tempting to speculate that the ESR reflects, to some extent, the condition of the inner blood vessel wall in the course of inflammatory processes.

In conclusion, the RBC surface "reports" on the surface of the vascular endothelium. Thus, a blood sample could give insight into the surface properties of endothelial cells.

Acknowledgments This work was supported by the Deutsche Forschungsgemeinschaft (Koselleck-grant OB 63/18). I am grateful to Ms. Marianne Wilhelmi for her excellent work in endothelial cell culture. I gratefully acknowledge the networking activities of COST Action TD 1002. The use of blood samples from volunteers was approved by the local Ethics Committee (Ärztekammer Westfalen-Lippe, approval number 2012-029-f-S).

Conflict of interest The author declares that he has no conflict of interest.

References

1. Becker BF, Chappell D, Jacob M (2010) Endothelial glycocalyx and coronary vascular permeability: the fringe benefit. Basic Res Cardiol 105:687–701
2. Binnig G, Quate CF (1986) Atomic force microscope. Phys Rev Lett 56(9):930–934
3. Curry FE, Adamson RH (2012) Endothelial glycocalyx: permeability barrier and mechanosensor. Ann Biomed Eng 40:828–839
4. Devaraj S, Yun JM, Adamson G, Galvez J, Jialal I (2009) C-reactive protein impairs the endothelial glycocalyx resulting in endothelial dysfunction. Cardiovasc Res 84:479–484
5. Drzeniek Z, Stocker G, Siebertz B, Just U, Schroeder T, Ostertag W, Haubeck HD (1999) Heparan sulfate proteoglycan expression is induced during early erythroid differentiation of multipotent hematopoietic stem cells. Blood 93:2884–2897
6. Durocher JR, Payne RC, Conrad ME (1975) Role of sialic acid in erythrocyte survival. Blood 45:11–20
7. Dvorak HF (2010) Vascular permeability to plasma, plasma proteins, and cells: an update. Curr Opin Hematol 17:225–229
8. Edgell CJ, Haizlip JE, Bagnell CR, Packenham JP, Harrison P, Wilbourn B, Madden VJ (1990) Endothelium specific Weibel–Palade bodies in a continuous human cell line, EA.hy926. In Vitro Cell Dev Biol 26:1167–1172
9. Gao L, Lipowsky HH (2010) Composition of the endothelial glycocalyx and its relation to its thickness and diffusion of small solutes. Microvasc Res 80:394–401
10. Godin C, Caprani A (1996) Interactions of erythrocytes with an artificial wall: influence of the electrical surface charge. Eur Biophys J 25:25–30
11. Hadengue AL, Del-Pino M, Simon A, Levenson J (1998) Erythrocyte disaggregation shear stress, sialic acid, and cell aging in humans. Hypertension 32:324–330
12. Hebbel RP, Moldow CF, Steinberg MH (1981) Modulation of erythrocyte–endothelial interactions and the vasocclusive severity of sickling disorders. Blood 58:947–952
13. Jan KM, Chien S (1973) Influence of the ionic composition of fluid medium on red cell aggregation. J Gen Physiol 61:655–668

14. Jan KM, Chien S (1973) Role of surface electric charge in red blood cell interactions. J Gen Physiol 61:638–654
15. Kliche K, Jeggle P, Pavenstadt H, Oberleithner H (2011) Role of cellular mechanics in the function and life span of vascular endothelium. Pflugers Arch 462:209–217
16. Kobayashi K, Kato K, Sugi T, Takemae H, Pandey K, Gong H, Tohya Y, Akashi H (2010) *Plasmodium falciparum* BAEBL binds to heparan sulfate proteoglycans on the human erythrocyte surface. J Biol Chem 285:1716–1725
17. Korte S, Wiesinger A, Straeter AS, Peters W, Oberleithner H, Kusche-Vihrog K (2012) Firewall function of the endothelial glycocalyx in the regulation of sodium homeostasis. Pflugers Arch 463:269–278
18. Kusche-Vihrog K, Urbanova K, Blanque A, Wilhelmi M, Schillers H, Kliche K, Pavenstadt H, Brand E, Oberleithner H (2011) C-reactive protein makes human endothelium stiff and tight. Hypertension 57:231–237
19. Lipowsky HH, Gao L, Lescanic A (2011) Shedding of the endothelial glycocalyx in arterioles, capillaries, and venules and its effect on capillary hemodynamics during inflammation. Am J Physiol Heart Circ Physiol 301:H2235–H2245
20. Liu M, Yang J (2009) Electrokinetic effect of the endothelial glycocalyx layer on two-phase blood flow in small blood vessels. Microvasc Res 78:14–19
21. Moncada S, Higgs EA (2006) Nitric oxide and the vascular endothelium. Handb Exp Pharmacol 213–254
22. Neu B, Sowemimo-Coker SO, Meiselman HJ (2003) Cell–cell affinity of senescent human erythrocytes. Biophys J 85:75–84
23. Noble MI, Drake-Holland AJ, Vink H (2008) Hypothesis: arterial glycocalyx dysfunction is the first step in the atherothrombotic process. QJM 101:513–518
24. Oberleithner H (2012) Two barriers for sodium in vascular endothelium? Ann Med 44(Suppl 1):S143–S148
25. Oberleithner H, Ludwig T, Riethmuller C, Hillebrand U, Albermann L, Schafer C, Shahin V, Schillers H (2004) Human endothelium: target for aldosterone. Hypertension 43:952–956
26. Oberleithner H, Peters W, Kusche-Vihrog K, Korte S, Schillers H, Kliche K, Oberleithner K (2011) Salt overload damages the glycocalyx sodium barrier of vascular endothelium. Pflugers Arch 462:519–528
27. Peters W, Drueppel V, Kusche-Vihrog K, Schubert C, Oberleithner H (2012) Nanomechanics and sodium permeability of endothelial surface layer modulated by hawthorn extract WS 1442. PLoS One 7:e29972
28. Pot C, Chen AY, Ha JN, Schmid-Schönbein GW (2011) Proteolytic cleavage of the red blood cell glycocalyx in a genetic form of hypertension. Cell Mol Bioeng 4:678–692
29. Pries AR, Secomb TW, Gaehtgens P (2000) The endothelial surface layer. Pflugers Arch 440:653–666
30. Pries AR, Secomb TW, Jacobs H, Sperandio M, Osterloh K, Gaehtgens P (1997) Microvascular blood flow resistance: role of endothelial surface layer. Am J Physiol 273:H2272–H2279
31. Reitsma S, Slaaf DW, Vink H, van Zandvoort MA, oude Egbrink MG (2007) The endothelial glycocalyx: composition, functions, and visualization. Pflugers Arch 454:345–359
32. Schneider SW, Matzke R, Radmacher M, Oberleithner H (2004) Shape and volume of living aldosterone-sensitive cells imaged with the atomic force microscope. Methods Mol Biol 242:255–279
33. Secomb TW, Hsu R, Pries AR (1998) A model for red blood cell motion in glycocalyx-lined capillaries. Am J Physiol 274:H1016–H1022
34. Serroukh Y, Djebara S, Lelubre C, Zouaoui BK, Biston P, Piagnerelli M (2012) Alterations of the erythrocyte membrane during sepsis. Crit Care Res Pract 2012:702956
35. Shiu YT, McIntire LV (2003) In vitro studies of erythrocyte–vascular endothelium interactions. Ann Biomed Eng 31:1299–1313
36. Stevens AP, Hlady V, Dull RO (2007) Fluorescence correlation spectroscopy can probe albumin dynamics inside lung endothelial glycocalyx. Am J Physiol Lung Cell Mol Physiol 293:L328–L335
37. Van Teeffelen JW, Brands J, Stroes ES, Vink H (2007) Endothelial glycocalyx: sweet shield of blood vessels. Trends Cardiovasc Med 17:101–105
38. Varez-Llamas G, Zubiri I, Maroto AS, de la CF, Posada-Ayala M, Martin-Lorenzo M, Barderas MG, Fernandez-Fernandez B, Ramos A, Ortiz A, Vivanco F (2012) A role for the membrane proteome in human chronic kidney disease erythrocytes. Transl Res 160:374–383
39. Vaziri ND (2004) Oxidative stress in uremia: nature, mechanisms, and potential consequences. Semin Nephrol 24:469–473
40. Versteeg HH, Heemskerk JW, Levi M, Reitsma PH (2013) New fundamentals in hemostasis. Physiol Rev 93:327–358
41. Vestweber D (2012) Novel insights into leukocyte extravasation. Curr Opin Hematol 19:212–217
42. Vink H, Wieringa PA, Spaan JA (1995) Evidence that cell surface charge reduction modifies capillary red cell velocity–flux relationships in hamster cremaster muscle. J Physiol 489(Pt 1):193–201
43. Vlahu CA, Lemkes BA, Struijk DG, Koopman MG, Krediet RT, Vink H (2012) Damage of the endothelial glycocalyx in dialysis patients. J Am Soc Nephrol 23:1900–1908
44. Vogt AM, Winter G, Wahlgren M, Spillmann D (2004) Heparan sulphate identified on human erythrocytes: a *Plasmodium falciparum* receptor. Biochem J 381:593–597
45. Weinbaum S, Tarbell JM, Damiano ER (2007) The structure and function of the endothelial glycocalyx layer. Annu Rev Biomed Eng 9:121–167
46. Weinbaum S, Zhang X, Han Y, Vink H, Cowin SC (2003) Mechanotransduction and flow across the endothelial glycocalyx. Proc Natl Acad Sci U S A 100:7988–7995
47. Wildling L, Hinterdorfer P, Kusche-Vihrog K, Treffner Y, Oberleithner H (2008) Aldosterone receptor sites on plasma membrane of human vascular endothelium detected by a mechanical nanosensor. Pflugers Arch 458(2):223–3
48. Zeng Y, Ebong EE, Fu BM, Tarbell JM (2012) The structural stability of the endothelial glycocalyx after enzymatic removal of glycosaminoglycans. PLoS One 7:e43168